

A comparison between the 'coil-to-globule' transition of linear chains and the "volume phase transition" of spherical microgels†

Chi Wu*

The Open Laboratory of the Bond Selecting Chemistry, Department of Chemical Physics, University of Science and Technology of China, Hefei, Anhui, China

(Received 2 May 1997; revised 12 September 1997; accepted 15 September 1997)

The coil-to-globule transition of individual poly(N-isopropylacrylamide) (PNIPAM) linear chains and the volume phase transition of spherical PNIPAM microgels were studied by a combination of static and dynamic laser light scattering. The thermodynamically stable collapsed single-chain globule was observed for the first time. The ratio of R_g/R_h lower than 0.774, predicted for a uniform sphere, indicates that the coil-to-globule transition is not an 'all-or-nothing' process, where R_g and R_h are the gyration and hydrodynamic radii, respectively. The time scale less than 100 s observed in the coil-to-globule transition is too short to support a suggested high chain-knotting density inside the globule. At the collapsing limit, the single-chain globule and microgel particle still contain 80% and 70% of water respectively in their hydrodynamic volumes. As for the volume phase transition, our results indicated that the volume change of the microgels is practically continuous, in contrast to the discontinuous volume phase transition observed in bulk PNIPAM gels. The discrepancy between a microgel and a bulk gel can be attributed to shear modulus. © 1998 Elsevier Science Ltd. All rights reserved.

(Keywords: coil-to-globule transition; volume phase transition; spherical microgels)

INTRODUCTION

Three decades ago, it was suggested that a flexible polymer chain can change from an expanded coil to a collapsed globule¹. Since then, this prediction was studied extensively both theoretically and experimentally^{2–11}. Most past studies concentrated on polystyrene solutions, satisfying the requirement of a very high molar mass and narrow molar mass distribution in the study of coil-to-globule transition. Useful experimental results were obtained using static and dynamic laser light scattering (LLS)^{8–11} and interpreted by the existing theory^{4–6}.

Three years ago, Grosberg and Kuznetsov¹² concluded that the true equilibrium single chain collapse had not yet been observed experimentally for simple uncharged homopolymers without mesogenic groups on the basis of numerous unsuccessful tries in many laboratories. In their article, they withdraw from the thermodynamic stable globular state by asking

- (1) Is it possible to reach the globular state of chains in a nonequilibrium polymer solution before precipitation?
- (2) What type of globular state can be realized under nonequilibrium conditions? Is it the crumpled globule or the knotted one?
- (3) What is the dynamics of a dilute polymer solution initiated by fast cooling from good-solvent temperature?

They predicted a two-stage kinetic for the collapse of a single chain, a fast crumpling of the unknotted chain

followed by a slow knotting of the collapsed polymer chain. This two-stage kinetic has recently been observed by Chu *et al.*^{13,14} in a kinetic study of the collapse of single polystyrene chain before precipitation. In their experiment, dynamic LLS was employed to monitor the change of the hydrodynamic radius (R_h) of a single polystyrene chain in cyclohexane after an abrupt temperature change from 35°C (the Θ -temperature of polystyrene in cyclohexane) to 29°C. Their measured hydrodynamic radius distribution showed two quite different species which were attributed to individual polystyrene chains and the aggregates. From the time dependence of R_h , two relaxation times t_{crum} and t_{eq} , respectively for the crumpled globule and compact globule states, were reported.

The interest in this coil-to-globule transition is not only due to its importance as a fundamental concept in polymer physics and solution dynamics, but also due to its relevance to many biological systems, such as protein folding¹⁵ and DNA packing^{16–18}. Therefore, the investigation of the coil-to-globule transition of polymers in aqueous solution is most interesting. In contrast, the study of aqueous polymer solutions often involves additional interaction, making theoretical development more difficult. Only a very limited number of studies have been reported^{19–21}. All of them involve poly(N-isopropylacrylamide) (PNIPAM) in water.

The main driving forces for collapse of the PNIPAM chain in water are the hydrophobic and hydrophilic interactions, which are much stronger than the van de Waals interactions between the polystyrene chain in an organic solvent²². Therefore, it should be easier for individual PNIPAM chains to reach a collapsed state in water than for polystyrene chains in an organic solvent. Kubota *et al.*²⁰ were the first to attempt to use a narrowly distributed PNIPAM sample to study the coil-to-globule

* Correspondence address: Department of Chemistry, The Chinese University of Hong Kong, Shatin, N.T. Hong Kong, China.

† Dedicated to the 80th birthday of Professor Renyuan Qian.

transition in water and confirmed the existence of a lower critical solution temperature (LCST, $\sim 32.00^\circ\text{C}$). Three PNIPAM samples with $M > 4.10 \times 10^6 \text{ g mol}^{-1}$ and $M_w/M_n > 1.3$ were used, and a limited chain collapse before the system reached thermodynamical instability, i.e., phase separation and aggregation, was observed. Meewes *et al.*²¹ went further using a PNIPAM sample ($M_w \sim 7 \times 10^6 \text{ g mol}^{-1}$ and $M_w/M_n \sim 1.3$) with a surfactant added to prevent phase separation. However, the addition of surfactant shifted the LCST to a higher temperature ($\sim 35^\circ\text{C}$) and complicated the coil-to-globule transition.

In order to study true single chain properties, a great effort was spent in this study to prepare two very narrowly distributed ($M_w/M_n < 1.05$) high molar mass ($M_w > 10^7 \text{ g mol}^{-1}$) PNIPAM samples. It is well known that for a polydisperse sample, polymer chains with a higher molar mass will undergo the phase transition first, which leads to the solution into a thermodynamically unstable region. As expected, with our narrowly distributed high molar mass, water-soluble PNIPAM in extremely dilute solutions, we were able to see the coil-to-globule transition in a relatively wide temperature range, especially very near the phase transition temperature, but still in the one-phase region (thermodynamically stable). This is exactly why we were able to observe a thermodynamically stable PNIPAM globule for the first time and study the kinetics of the coil-to-globule transition in the thermodynamically stable region.

However, since Dusek and Patterson predicted the possibility of a discontinuous volume change of a polymer gel in analogy to the coil-to-globule transition²³, the volume phase transition of polymer gels has attracted much attention^{24–53}. Remarkable progress has been made in the understanding of the phase transitions and critical phenomena in polymer gels. It was reported that some polymer gels can swell or shrink discontinuously and reversibly in response to many different stimuli, such as temperature²⁸, pH²⁹, electric fields³⁰ or light³¹, depending on the chemical composition of a given gel/solvent system. The volume change can be as large as a thousand fold³². It was proposed to utilize the large volume change of polymer gels in response to an infinitesimal alternation in environment in controlled release of biological molecules at specific body conditions, selective absorbents, chemical memories, sensors and artificial muscles.

Several models were proposed to explain the volume phase transition. The earliest prediction of the collapse of the PNIPAM gel was made by Hirotsu *et al.*³⁵ and recently, they consider the concentration-dependence of the Flory interaction parameter (which can make the phase transition possible within the Flory–Huggins incompressible lattice model³⁶). However, this model cannot explain the experimental data in the collapsed regime since it neglects the volume changes of mixing and the topological constraints of the gel network. Marchetti *et al.*³⁸ introduced the lattice vacancy and finite chain extensibility to allow for a nonzero volume change of mixing, so that the data from larger deformation of the gels can be reasonably fitted. Considering the gel collapse as the coil-to-globule transition of subchains, Grosberg *et al.*³⁹ discussed the contribution of topological constraints to this process. Their theory can satisfactorily describe part of the results in the phase transition range. The diversity of theories shows that a better understanding of the volume phase transition of the PNIPAM gels is required.

So far, most experimental studies dealt with the swelling

and shrinking of bulk PNIPAM gels by using various methods, such as microscopy⁴⁰, dilatometry⁴¹, differential scanning calorimetry⁴², friction measurement⁴³, small angle neutron scattering⁴⁴ and NMR⁴⁵. Only very few studies of the PNIPAM microgels were reported^{46–49}. Tanaka *et al.*⁴² showed that for a spherical gel, the time required for swelling or shrinking is proportional to the square of its radius. Microgel particles with a small radius will have a much fast response to a change of its environment. The phase transition of gels is a macroscopic manifestation of the coil-to-globule transition of individual linear chains. Therefore, a comparison between the PNIPAM gel networks and individual PNIPAM linear chains in water will improve our understanding of swelling and shrinking at the molecular level.

In this study, nearly monodisperse spherical PNIPAM microgel particles ($R_h \sim 180 \text{ nm}$) were prepared by emulsion polymerization. The volume phase transition was studied by both static and dynamic laser light scattering. A comparison of the properties of the microgel particles with those of individual PNIPAM chains in water is presented.

THEORETICAL BACKGROUND

Collapse of a single chain

For a given polymer solution, the solvent can change from a good to a Θ -solvent and finally to a poor solvent, or *vice versa*, with temperature change. When the solvent quality is poor, a flexible polymer chain contracts. By using the modified Flory theory, the chain collapse was formulated in terms of an expansion factor $\alpha = R(T)/R(\Theta)$ by^{54,55}

$$\frac{7(1-\alpha^2)}{3r} = \frac{1}{2} \left(\frac{\Theta}{T} \right) \phi + \frac{\ln(1-\phi)}{\phi} + \quad (1)$$

where $\phi \equiv \phi_0/\alpha^3$ with ϕ_0 the fraction of space occupied by chains whose radius of gyration R_g is equal to the ideal value R_g^0 , r is the number of residues, which may be one monomer unit or a number of repeat units grouped together, and $R(T)$ and $R(\Theta)$ are the radius of gyration and hydrodynamic radius at temperature T and the Flory Θ -temperature, respectively. In equation (1), ϕ has to be less than one, i.e., $\alpha > \phi_0^{1/3}$. The maximum observed value of ϕ in this study was ~ 0.5 . If $r \rightarrow \infty$, $\phi \rightarrow (19/27)^{1/2} r^{-1/2}$. In a good solvent, $\alpha > 1$ and $\phi \ll 1$. Expanding $\ln(1-\phi)$, we can rewrite equation (1) in a more familiar form as⁵⁶

$$\alpha^6(1-\alpha^2) + 0.102 + \dots = 0.180\alpha^3\tau(M_w/M_0)^{1/2} \quad (2)$$

where $\tau = [(T-\Theta)/\Theta]$ is the reduced temperature, $[(T-\Theta)/T]$ is approximated by τ since T is near Θ , and we have replaced r by (M_w/M_0) , with M_w and M_0 being the molar masses of the polymer and that of the 'residues', respectively. equation (2) shows that as α decreases $\alpha^3 M_w^{1/2} \tau$ approaches a plateau since the higher order terms can be dropped at small α and M_0 is independent of temperature. Moreover, equation (2) shows that $\alpha^3 M_w^{1/2} \tau$ is a function of $M_w^{1/2} \tau$.

Kinetics of the coil-to-globule transition

In comparison with the theoretical development of equilibrium single chain globule, few theoretical predictions have been published on the kinetics of the coil-to-globule transition. The proposed theories are either qualitative descriptions¹² or computer simulations with a limited chain length⁵⁷. One decade ago, de Gennes⁵⁸ stated that if

a polymer chain is quenched in a poor solvent the polymer chain will adopt a 'sausage'-like conformation wherein each block of 'sausage' will gradually shorten and thicken in a self-similar manner during the chain collapse. Using the solvent viscosity, the estimate of the characteristic relaxation time is in the order of $\sim 10^{-3}$ s, much shorter than the experimental value ($\sim 10^2$ s)¹⁴. This discrepancy may be attributed to a higher local viscosity when the polymer chain is collapsed and/or to possible topological constraints, such as self-entanglements in the globule, which will certainly slow down the kinetics.

On the basis of the above concepts, Grosberg *et al.*⁵⁹ qualitatively predicted that the collapse could be a two-stage process, i.e., a fast process similar to that described by de Gennes and a slow process assumed to be similar to self-repetition. The fast collapse could be visualized as crumpling, followed by a slow knotting process. In the first process, the chain density in its occupied volume increases fast as the chain collapses, while in the second process the increase of the chain density is much slowly due to the rearrangement of the collapsed chain in the globule. The relaxation times, i.e., τ_{crum} and τ_{eq} , associated with these processes can be written as^{12,14}

$$\tau_{\text{crum}} \propto M_w \left(\frac{2\eta}{\Theta} \right) \left(\frac{\alpha_{\text{crum}}}{\alpha_{\text{eq}}} \right)^3 \quad (3)$$

and

$$\tau_{\text{eq}} \propto M_w \left(\frac{3\eta}{\Theta} \right) \gg \tau_{\text{crum}} \quad (4)$$

where η is the solvent viscosity and the ratio of the expansion factors ($\alpha_{\text{crum}}/\alpha_{\text{eq}}$) is related to the size ratio,

$$\alpha_{\text{crum}}/\alpha_{\text{eq}} \propto g = R_{\text{crum}}/R_{\text{eq}} = (1 + \zeta) \quad (5)$$

where ζ is a constant. Practically, it is rather difficult to verify this two-stage collapse because the time for the polymer solution to reach a temperature equilibrium after a temperature jump is longer than the relaxation times. This is why only one experimental result has been reported so far¹⁴.

Volume phase transition of polymer gels

The swelling (or shrinking) of polymer gels is a fundamental and classic problem in polymer physics. A three-dimensional crosslinked polymer network filled with small solvent molecules in its interstitial space provides a model system for the study of an viscoelastic body. Flory^{60,61}, Hermans⁶² and James-Guth⁶³ have presented several models to calculate the free energy change related to the swelling or shrinking of a polymer gel. On the basis of these models, Dusek *et al.*^{23,64} have shown that certain polymer gels can undergo a discontinuous volume change (a volume phase transition) as temperature changes after considering the chemical potential of the solvent in equilibrium with the swollen gel, namely

$$\Delta\mu_1/RT = \ln a_1 = \ln(1 - \varphi_2) + \varphi_2 + \chi_T \varphi_2^2 + \zeta(\varphi_2^{1/3} \langle \alpha^2 \rangle_0 - \kappa \varphi_2) \quad (6)$$

and the chemical potential per equivalent segment of the network polymer,

$$\Delta\mu_2/nRT = -\varphi_1 + \chi_T \varphi_1^2 + \zeta[\langle \alpha^2 \rangle_0 (\varphi_2^{-2/3}/2 + \varphi_2^{-1/3} - 3/2) - \kappa(\ln \varphi_2 + \varphi_1)] \quad (7)$$

where the subscripts 1 and 2 denote the solvent and the polymer, respectively, $n = V_2/V_1$ with V being the partial molar volume, φ is the volume fraction, χ_T is the Flory-Huggins polymer-solvent interaction parameter depending on the temperature T . $\zeta = \rho V_1/M_c$, where ρ and M_c are respectively the density of the dry gel and the average molar mass of the subchain between two neighbour crosslinking points. $\langle \alpha^2 \rangle_0$ is the isotropic deformation factor of the gel network and is defined as the ratio of the mean-square end-to-end distance of the chains in a dry network to the value of unperturbed free chains; and $0 < \kappa < 1$ depending on the models⁶¹⁻⁶³.

When two phases of the different concentrations coexist, the two equations $\mu_1 = \mu_1'$ and $\mu_2 = \mu_2'$ have a solution outside the unstable region wherein $\partial\Delta\mu_2/\partial\varphi_2 > \partial\Delta\mu_1/\partial\varphi_2$. Inserting equations (1) and (2) into $\mu_1 = \mu_1'$ and $\mu_2 = \mu_2'$, one can calculate the curves describing the composition of the gel, namely χ_T versus φ_2 . The coexistence of the swollen and the collapsed phases requires that χ_T is sufficiently high, and at the same time $\langle \alpha^2 \rangle_0$ and M_c are sufficiently low. However, a low M_c means a high-crosslinking density or a high $\langle \alpha^2 \rangle_0$. Therefore, it is more practical to choose a gel system with a strong interaction between the polymer network and solvent, i.e., a higher χ_T , to study the volume phase transition.

This rational prediction has stimulated considerable efforts to study the volume phase transition of a pure binary polymer/solvent gel system where hydrogels were normally chosen because of their higher χ_T values. A number of studies on certain lightly crosslinked poly(N-isopropylacrylamide) (PNIPAM) gels have shown a very sharp volume change at $\sim 33^\circ\text{C}$ which was considered as the discontinuous volume phase transition^{46,65-69}. However, a continuous volume change was also observed for the PNIPAM and other hydrogels^{42,70-72}. It is worth noting that Li and Tanaka⁴² have shown that by the decrease of the crosslinking density of a bulk PNIPAM gel can lead a continuous volume change to a discontinuous one. On the basis of equations (6) and (7), a discontinuous volume phase transition should exist as long as the two equations $\mu_1 = \mu_1'$ and $\mu_2 = \mu_2'$ have a solution outside the unstable region.

Microscopically, there is an analogous between the 'coil-to-globule' transition of a single linear polymer chain and the volume phase transition of a swollen polymer gel. The swelling or shrinking of a polymer gel is caused by the expansion or contraction of the subchains between two neighbouring crosslinking points inside the gel network. Therefore, a comparison study of the 'coil-to-globule' transition of a single linear polymer chain and a crosslinked polymer gel can lead to a better understanding of the swelling/shrinking of polymer gels.

Laser light scattering (LLS)

In static LLS, for a dilute solution or colloidal dispersion at a small scattering angle the weight-average molar mass M_w , the average radius of gyration $\langle R_g^2 \rangle$ (written as $\langle R_g \rangle$), and the second virial coefficient A^2 can be related to the excess absolute time-averaged scattered light intensity (the Rayleigh ratio $[R_v(q)]$)^{73,74}. In dynamic LLS, a precise intensity-intensity time correlation function $G^{(2)}(t, q)$ in the self-beating mode can be measured^{75,76}, which can lead to the line-width distribution $G(\Gamma)$, where the line-width Γ is usually a function of both C and θ ⁷⁷. $G(\Gamma)$ can be obtained from the Laplace inversion of $G^{(2)}(t, q)$. If the relaxation is diffusive, Γ/q^2 equals the translational diffusion coefficient D at $c \rightarrow 0$ and $q \rightarrow 0$. In this case, $G(\Gamma)$ can be converted to

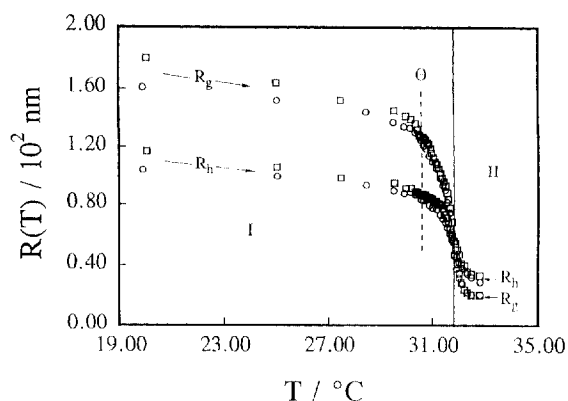


Figure 1 Temperature dependence of the PNIPAM chain dimension, where 'O' represents both the radius of gyration R_g and the hydrodynamic radius R_h for PNIPAM-1, and '□', for PNIPAM-2. The dashed line indicates the Flory Θ -temperature. The thermodynamically stable one-phase and kinetically stable two-phase region are respectively denoted as I and II⁸⁵

the translational diffusion coefficient distribution $G(D)$ or to the hydrodynamic radius distribution $f(R_h)$ by $R_h = k_B T / (6\pi\eta D)$, where k_B and η are the Boltzmann constant and solvent viscosity, respectively.

EXPERIMENTAL

Sample preparation

N-isopropylacrylamide (courtesy of Kohjin, Ltd, Japan) was recrystallized three times in a benzene/n-hexane mixture. N,N'-methylenebis(acrylamide) (BIS) as a cross-linker was recrystallized from methanol. Potassium persulfate (KPS) (from Aldrich, analytical grade) as an initiator and sodium dodecyl sulfate (SDS) (from BDH, 99%) as a dispersant were used without further purification. The details of the PNIPAM preparation were as described earlier^{78,79}. A careful combination of both the fractionation and filtration enabled us to prepare two very narrowly distributed ($M_w/M_n < 1.05$) high molar mass PNIPAM samples. Hereafter, they are denoted as PNIPAM-1 ($M_w = 1.08 \times 10^7 \text{ g mol}^{-1}$) and PNIPAM-2 ($M_w = 1.21 \times 10^7 \text{ g mol}^{-1}$). With these PNIPAM samples, we prepared and clarified the extremely dilute PNIPAM aqueous solutions ($C \sim 5 \times 10^{-6} \text{ g mL}^{-1}$) with a 0.5 mm filter. The resistivity of the distilled deionized water used as solvent in this study was 18.3 M Ω cm. The PNIPAM microgels were made by emulsion polymerization⁸⁰. The microgel particles were purified and diluted to $\sim 10^{-5} - 10^{-6} \text{ g mL}^{-1}$ for further LLS measurements.

LLS instrumentation

A commercial LLS spectrometer (ALV/SP-150) equipped with an ALV-5000 digital time correlator was used with a solid-state laser (ADLAS DPY425II, output power $\approx 400 \text{ mW}$ at $\lambda = 532 \text{ nm}$) as the light source. The incident light was vertically polarized with respect to the scattering plane and the light intensity was regulated with a beam attenuator (Newport M-925B) to avoid a possible localized heating in the light-scattering cuvette. In our set-up, the coherent factor β in dynamic LLS is ~ 0.87 . With some proper modifications⁸¹, our LLS spectrometer is capable of recording both static and dynamic LLS continuously in the range 6–154°. The accessible small angle range is particularly useful in the measurement of large microgel particles because the condition of $qR_g < 1$ is required to determine M_w , R_g and D .

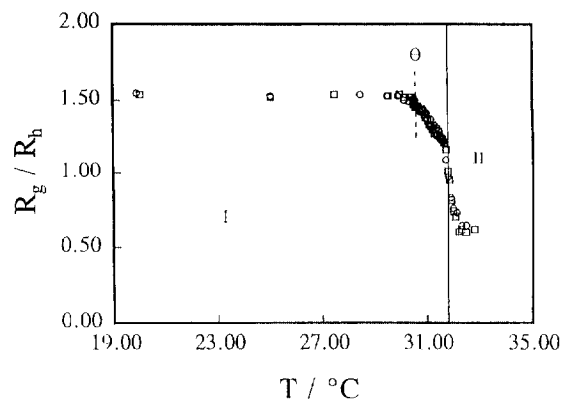


Figure 2 Temperature dependence of R_g/R_h , where all symbols have the same meanings as in Figure 1⁸⁵

RESULTS AND DISCUSSION

The 'coil-to-globule' transition of individual PNIPAM chains

Figure 1 shows the PNIPAM chain dimension R as a function of the solution temperature, where 'O' represents both the radius of gyration R_g and the hydrodynamic radius R_h for PNIPAM-1, and '□' for PNIPAM-2. The regions I and II refer to the thermodynamically stable one-phase region and kinetically stable two phase region, i.e., in region II individual PNIPAM chains first collapsed to densely packed single-chain globules which were only stable for a limited time period ($\sim 10^2 \text{ min}$) and then the globules were thermodynamically driven towards aggregation so that the system entered a two-phase region. Figure 1 shows that in the region of $T < \Theta$ the chain slightly shrinks as temperature increases and both R_g and R_h are linear functions of temperature. When $T > \Theta$, the PNIPAM chain starts to collapse and both R_g and R_h decrease dramatically as T is distant from Θ . Figure 1 also shows that when the temperature increases from 20°C to 33°C the PNIPAM chain dimension in terms of R_g decreases ~ 8 times, whereas the decrease of R_h is only ~ 3.5 times in the same temperature range. This difference between the changes of R_g and R_h is understandable because they are defined in quite different ways. R_g is related to the actual space reached by the polymer chain, while R_h is only the radius of an equivalent hard sphere which has an identical diffusion coefficient D as the polymer chain in the solution. When the polymer chain is an extended coil, the water molecules in its occupied space are draining when the polymer chain diffuses, so that R_h is much smaller than R_g , while in the collapsed state, the water molecules inside the globule are less draining so that R_g decreases fast.

Figure 2 shows R_g/R_h as a function of the temperature, where all symbols and labels have the same meanings as in Figure 1. Figure 2 shows that the plots of R_g/R_h versus T for two different molar masses have collapsed into a single line, which is expected because R_g/R_h depends only on the chain conformation, not on the molar mass, as predicted and experimentally verified^{76,77}. Figure 2 shows that when $T < \Theta$, R_g/R_h is a constant (~ 1.52), even though both R_g and R_h decrease with increasing T as shown in Figure 1. The value of ~ 1.52 is close to the predicted value for a flexible coil in a good solvent, which means that when $T < \Theta$ the PNIPAM chain in water behaves like a random coil and the conformation is independent of temperature. Figure 2 shows also that when $T > \Theta$, R_g/R_h first decreases linearly with temperature increases and then drops just

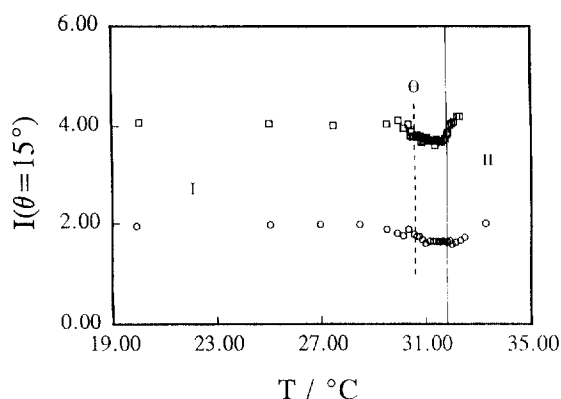


Figure 3 Temperature dependence of the scattered light intensity $I(\theta = 15^\circ)$, where all symbols and labels have the same meanings as in Figure 1⁸⁵

before entering the two-phase region II. A combination of Figures 1 and 2 shows that the linear decrease of R_g/R_h in this region is mainly due to the fast decrease of R_g . We attribute this linear decrease of R_g/R_h to the chain crumpling process, whereby a polymer chain contracts towards its centre and the chain segments at the centre and near the surface of the globule should contract simultaneously, leading to the decrease of R_g , while R_h is mainly affected by the contraction near the surface. As the chain contracts, the chain density increases and most of the water molecules inside the collapsed chain will be nondraining. Therefore, the collapsed chain with the water molecules caged inside will become more and more like a hard sphere. R_h should gradually approach to the dimension of the collapsed chain and the decrease of R_h will slow down. At present, it is not clear why R_g/R_h decreases linearly with temperature in that region. At $T \approx 32^\circ\text{C}$ where $R_g \approx R_h$, the PNIPAM solution entered the two-phase region II. In this region, R_g and R_h were measured in the kinetically stable state, namely before the aggregation of the collapsed globules. In the kinetically stable region II, R_g/R_h dropped from ~ 1 to a plateau value of ~ 0.63 . It is worth noting that R_g/R_h has dropped below 0.774, predicted for a uniform sphere. In the past, this value was repeatedly taken as a criterion to check whether a given polymer chain has reached a globule state with a uniform density^{9,20,21}. The plateau value (~ 0.62) indicates that the density of the globule is not uniform, namely the centre of the chain contracts faster than those near the surface, resulting a higher density in the centre of the globule. This observation indicates that the coil-to-globule transition is

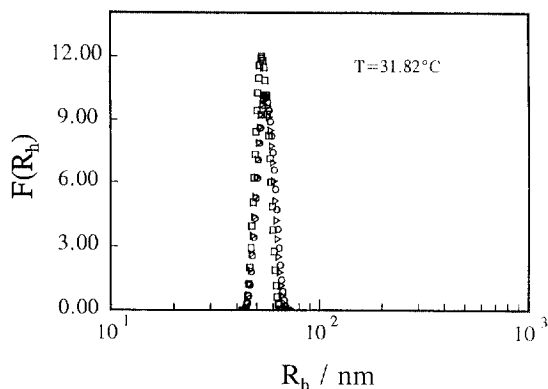


Figure 4 Hydrodynamic radius distribution $f(R_h)$ of PNIPAM-1 at different standing times after the solution was brought from 30.59°C (the Θ -temperature) to 31.82°C (in Region I), where 'O', $t = 5$ h, ' Δ ', 33 h, and ' \square ', 44 h⁸⁵

not an all-or-nothing process⁸². It should be noted that this lower plateau value can also be seen in Figure 4 of Kubota *et al.*²⁰, where it was overlooked.

Figure 3 shows the scattered light intensity $I(\Theta = 15^\circ)$ as a function of temperature, where all symbols and labels have the same meanings as in Figure 1. According to equation (6), $I(q)$ at a fixed scattering angle should be nearly independent of temperature as long as there is no change in M_w and C , where we have assumed that n and dn/dC do not change too much in the small temperature range. This independent of $I(q)$ on temperature is shown in Figure 3. However, when $T > \Theta$, in Region I, $I(q)$ starts to decrease. First, we were astonished by this unexpected and strange intensity decrease since if there is aggregation $I(q)$ should increase. This cannot be explained by the possible change of dn/dC , R_g or A_2 according to equation (1), because in the PNIPAM chain collapse, R_g decreases, A_2 becomes more negative, and dn/dC (if there are any changes) might increase slightly. Eventually, we speculated that the decrease of $I(q)$ may be attributed to the multiple scattering inside the collapsed PNIPAM globule in which the microscopic concentration is higher even though the macroscopic concentration is very low. The light scattered from the segments located at the centre of the chain might be blocked by the segments near the surface when the scattered light travels from the chain centre to the surface. Nevertheless, Figure 3 shows that in the region I PNIPAM is thermodynamically stable in water and there is no aggregation between the PNIPAM molecules. On the other hand, in Region II, $I(q)$ increases with temperature, indicating aggregation of the collapsed single-chain globules. LLS is an extremely sensitive method to detect aggregates in a given polymer solution because $I(q)$ is directly proportional to the square of the mass M of the scatterer. Thus, Figure 3 supports our previous claim that the PNIPAM solution is thermodynamically stable in Region I, while the solution is only kinetically stable in Region II. This can be further demonstrated by our dynamic LLS results.

Figure 4 shows the hydrodynamic radius distribution $f(R_h)$ of PNIPAM-1 at different times (t) after the solution was brought from 30.59°C (the Θ -temperature) to 31.82°C (still in the thermodynamically stable region). In terms of the distribution width and peak position, the independence of $f(R_h)$ on time indicates that the PNIPAM in water at $T = 31.82^\circ\text{C}$ is thermodynamically stable. Moreover, $f(R_h)$ shows that the PNIPAM used in this study is narrowly distributed. In contrast, when $T > 32.01^\circ\text{C}$, we saw a very slow aggregation process.

Figure 5 shows a typical slow aggregation process (in terms of $f(R_h)$) after the same solution used in Figure 4 was brought from 30.59°C to 33.02°C . No aggregation can be detected up to $t = 1850$ s. Only after standing at 33.02°C for ~ 1 h, $f(R_h)$ was gradually broadened. When $t \sim 3.44$ h, a very small second peak appeared in $f(R_h)$ represented a very small amount of the larger aggregates presumably made of individual collapsed single-chain globules. We found that the aggregation rate slows down as temperature approaches to $\sim 32^\circ\text{C}$. After a set of careful experiments, we concluded that the phase transition temperature for the PNIPAM solution was $\sim (32.00 \pm 0.05)^\circ\text{C}$. Next, we will present the kinetic studies of the coil-to-globule transition of individual PNIPAM chains in water.

Figure 6 shows the dissolving kinetics (in terms of R_h) of the highly collapsed single-chain globule, where t is the standing time after the solution temperature was quenched

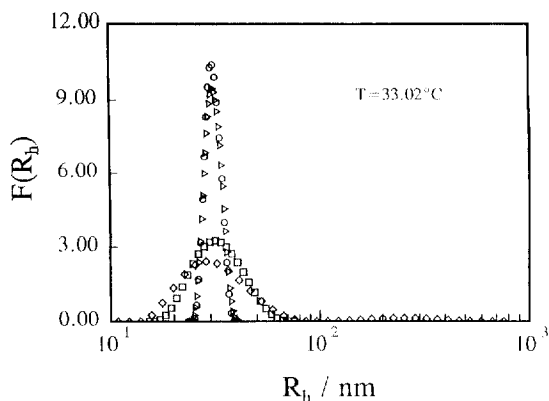


Figure 5 Typical slow aggregation process (in terms of $f(R_h)$) after the same PNIPAM solution used in *Figure 4* was brought from 30.59°C to 33.02°C, where 'O', $t = 280$ s, 'Δ', 1850 s, '□', 3690 s, and '◇', 3.44 h⁸⁵

from 33.02°C to 30.02°C. The experimental procedure was as follows. First, the value of R_h at 30.02°C was determined (the dashed line in *Figure 6*). Then, the solution temperature was increased to 33.02°C and stayed at 33.02°C for ~ 10 s before the temperature quenching. In this way, individual PNIPAM chains only had enough time to collapse, but no time to aggregate with each other (as shown in *Figure 5*). Both R_g and t were immediately recorded after the temperature quenching. The insert in *Figure 6* shows how fast the solution temperature was able to reach the equilibrium value, wherein a very special LLS cuvette made of a thin wall (~ 0.4 mm) glass tube was used for all kinetic studies. *Figure 6* shows that the melting process (the globule-to-coil process) is too fast to be followed in our present LLS set-up, i.e., before the solution reached its temperature equilibrium at 30.02°C the collapsed PNIPAM globule already 'melted' into a polymer coil. This fast melting time ($< \sim 100$ s) implies no extensive chain knotting inside the globule.

Figure 7 shows the kinetics of the coil-to-globule transition, where the temperature of the PNIPAM-1 solution was jumped from 30.59°C respectively to 31.82°C and 33.02°C and it took ~ 300 s to reach the temperature equilibrium. In the case of jumping from 30.59°C to 33.02°C (already inside Region II), the collapse was too fast to be followed. This fast collapsing process further indicates that no extensive knotting exists in the collapsed globule because the knotting cannot be so fast inside the collapsed

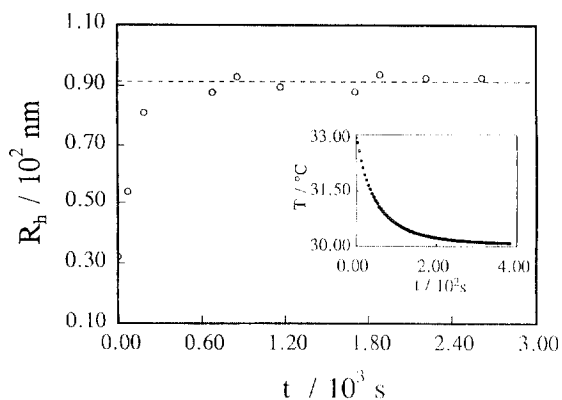


Figure 6 Kinetics of the globule-to-coil transition of single-chain (PNIPAM-1) globules, where t is the standing time after the solution temperature was quenched from 33.02°C to 30.02°C and the dashed line represents the thermodynamically stable size of the PNIPAM-1 coil at 30.02°C⁸⁵

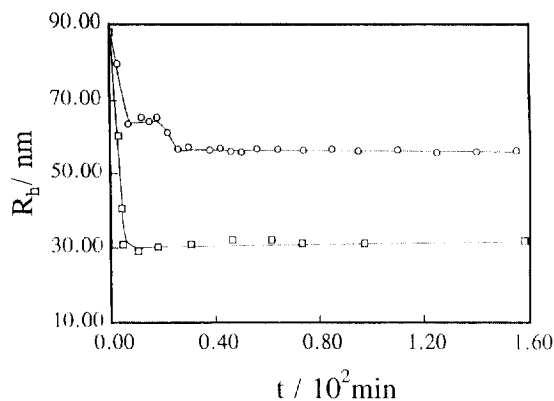


Figure 7 Kinetics of the coil-to-globule transition of the PNIPAM-1 chains after the temperature was jumped from 30.59°C respectively to 31.82°C ('O') and 33.02°C ('□'), where the lines were drawn simply for eye-guiding³⁵

globule. When the temperature jumped to 31.82°C (still in Region I), the chain collapse (the decrease of R_h) followed a very interesting two-stage process. The first stage is too fast to be accurately recorded, so that it would be difficult for us to quantitatively analyze the data in *Figure 7*. The estimated time scales for these two stages are ~ 50 and ~ 300 s, respectively. To our knowledge, this is the first time that two-stage collapsing kinetics was ever observed in the thermodynamically stable region. We might attribute the first stage as a simple contraction of the PNIPAM chain, which can be considered as a simple shrinking of the extended coil so that most of the existing topological constraints at 30.59°C were 'frozen' inside the contracted coil whose conformation might not be thermodynamically stable at 31.82°C, so that the PNIPAM chain has to relax into a thermodynamically stable conformation at 31.82°C by a possible crumpling predicted by Grosberg *et al.*¹². In comparison with the collapsed globule at 33.02°C, the thermodynamically stable globule at 31.82°C is twice-time large. If taking the value of R_h at 31.82°C and 33.02°C respectively as R_{crum} and R_{eq} in equation (5), we are able to obtain that $\zeta \sim 4.6$ which is smaller than the reported data (7–11) for polystyrene in cyclohexane^{9,12,14}.

Figure 8 shows a plot of the static expansion factor α_s as a function of the relative temperature Θ/T , where α_s is defined as $R_g(T)/R_g(\Theta)$. When $T < \Theta$ the experimental results are reasonably represented by the line with $r = 10^5$. A similar result was observed for polystyrene in cyclohexane^{19,81}. The

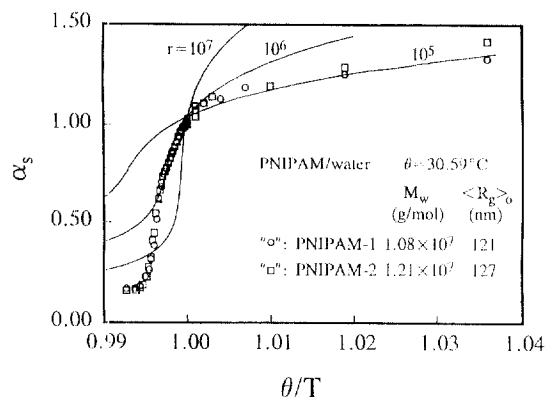


Figure 8 Plot of the static expansion factor α_s as a function of the relative temperature Θ/T , where α_s is defined as $R_g(T)/R_g(\Theta)$, 'O' (PNIPAM-1) and '□' (PNIPAM-2) are the measured results, and the lines, the calculated data from equation (1) with three different r values. If choosing $M_0 = 113$ (the mass of the repeat unit), we have $r \sim 10^5$ for PNIPAM-1 and PNIPAM-2⁸⁵

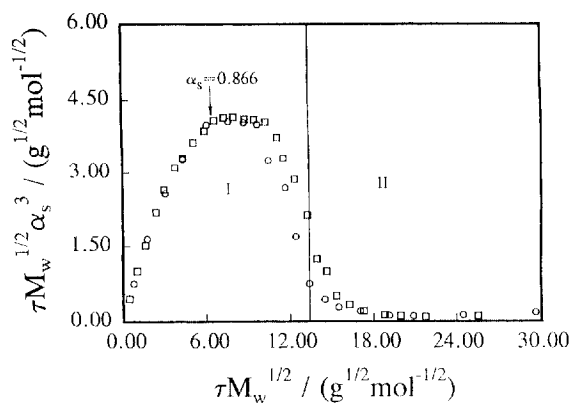


Figure 9 Plots of the scaled static expansion factor $\alpha_s^3 \tau M_w^{1/2}$ as a function of the reduced temperature $\tau M_w^{1/2}$ at $T > \Theta$ for PNIPAM-1 (\circ) and PNIPAM-2 (\square) in water⁸⁵

theory works well when the solvent is good wherein ϕ_0 is expected to be a weak function of T . However, when $T > \Theta$, the measured α_s drops much faster than the line with $r = 10^5$. We do not understand this discrepancy. Apparently, the results can be partially fitted by the line with $r = 10^6$. Another point is that α_s decreases to a much lower plateau than predicted in equation (1), which might be because the hydrophobic and hydrophilic interactions in water are much stronger than those predicted by theory.

Figures 9 and 10 respectively show the plots of the scaled expansion factor $\alpha_s^3 \tau M_w^{1/2}$ and $\alpha_h^3 \tau M_w^{1/2}$ as a function of $\tau M_w^{1/2}$. Such plots were reported before for polystyrene in organic solvents and also for PNIPAM in water^{7,15}. Several points in Figures 9 and 10 should be noted. We observed a well-established plateau for each of the PNIPAM samples. The plateau values in Figure 10 are very close to ~ 0.6 estimated from equation (2), but the plateau values in Figure 9 are $\sim 50\%$ lower. The ratio of the plateau values in Figures 10, and 9 is ~ 1.45 , much lower than $(1.481/1.161)^3 \sim 2$ predicted before²⁰, but close to the experimental values (~ 1.44) for polystyrene in various of organic solvents⁷. Also, $\alpha_s^3 \tau M_w^{1/2}$ drops at higher $\tau M_w^{1/2}$ (still in Region I), contradicting the prediction of equation (2). This paradox leads us to reexamine the conditions on which equations (1) and (2) were derived. In equations (1) and (2), the change of the attractive interactions is not included. The attractive interaction between different segments in a highly collapsed globule should be much stronger than that in the extended coil conformation. This might explain why there is a drop followed by a plateau and might also be the reason

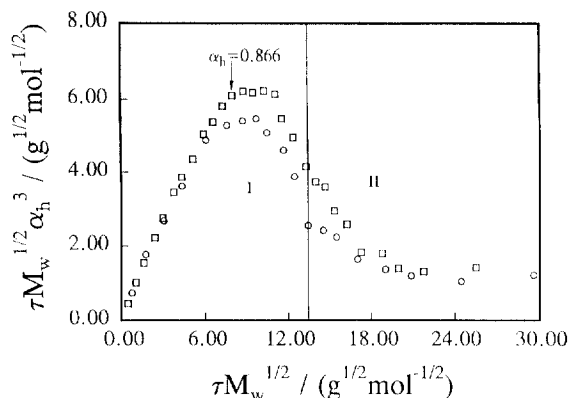


Figure 10 Plots of the scaled hydrodynamic expansion factor $\alpha_h^3 \tau M_w^{1/2}$ as a function of the reduced temperature $\tau M_w^{1/2}$ at $T > \Theta$ for PNIPAM-1 (\circ) and PNIPAM-2 (\square) in water, where $\alpha_h = R_h(T)/R_h(\Theta)$ ⁸⁵

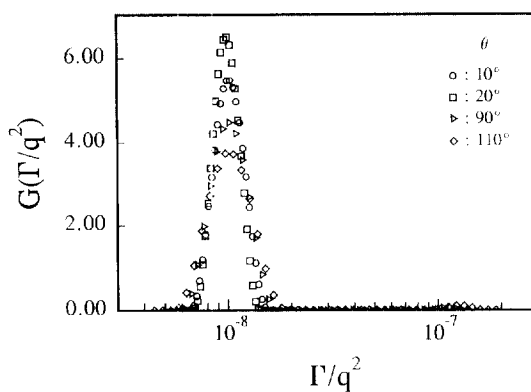


Figure 11 Line-width distributions $G(\Gamma/q^2)$ of the PNIPAM microgel particles in water at different scattering angles, where $T = 15^\circ\text{C}$ and $C = 1.182 \times 10^{-5} \text{ g mL}^{-1}$ ⁸⁰

for the fast decay in Figure 8 after $T > \Theta$. According to equation (2), when $d(\alpha^3 \tau M_w^{1/2})/d\alpha \sim 6\alpha^5 - 8\alpha^7 = 0$, i.e., $\alpha = 0.87$, the scaled expansion factor $\alpha^3 \tau M_w^{1/2}$ should reach a maximum, as shown in Figures 9 and 10, indicating that equation (2) works quite well until the plateau is reached.

Next, a combination of static and dynamic LLS results can lead to the chain density of the globule. Using a simple approximation of $\rho \sim M_w/[N_A(4/3)\pi R_h^3]$, we found that even in the mostly collapsed globule where $R_g/R_h \sim 0.62$ the estimate of the chain density ρ is only $\sim 0.2 \text{ g cm}^{-3}$, implying that the PNIPAM globule still contains $\sim 80\%$ of water.

The volume phase transition of spherical PNIPAM microgels

Figure 11 shows the angular dependence of the characteristic line-width distributions $G(\Gamma/q^2)$ of the PNIPAM microgels, where $C = 1.18 \times 10^{-5} \text{ g mL}^{-1}$ and $T = 15^\circ\text{C}$. When $\theta \leq 20^\circ$, only one peak with $\langle \Gamma \rangle / q^2 \sim 9.95 \times 10^{-9} \text{ cm}^2 \text{ s}^{-1}$ was observed. This peak is related to the translational diffusion of the microgel particles in water, from which we can calculate the hydrodynamic radius distribution $f(R_h)$. When $\theta \geq 90^\circ$, a very small second peak (barely seen in Figure 1) appears at $\langle \Gamma \rangle / q^2 \sim 1.45 \times 10^{-7} \text{ cm}^2 \text{ s}^{-1}$. This small second peak reflects the internal motion of the PNIPAM subchains between two neighbour crosslinking points. The first peak is very narrow and nearly independent of θ in the range of $8^\circ < \theta < 110^\circ$. This angular independence indicates a spherical symmetry of the microgel particles. The average hydrodynamic radius $\langle R_h \rangle$ of the PNIPAM microgels is $190 \pm 5 \text{ nm}$ at $T = 15^\circ\text{C}$.

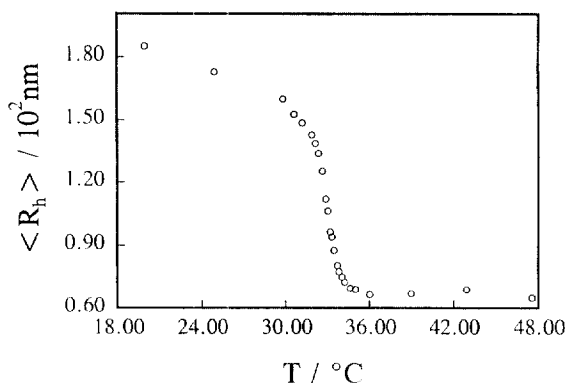


Figure 12 Average hydrodynamic radius $\langle R_h \rangle$ of the PNIPAM microgel particles as a function of the solution temperature⁸⁰

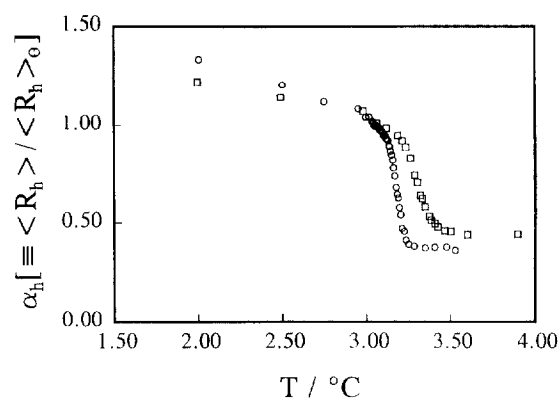


Figure 13 Expansion factor $\alpha_h[\equiv \langle R_h \rangle / \langle R_h \rangle_\Theta]$ as a function of temperature for the PNIPAM microgel particles and individual chains ($M_w = 1.08 \times 10^7 \text{ g mol}^{-1}$ and $M_z/M_w \sim 1.05$), where $\langle R_h \rangle_\Theta$ is the average hydrodynamic radius at $T = \Theta$

Figure 12 shows typical temperature dependence of the average hydrodynamic radius ($\langle R_h \rangle$). When $T < 31^\circ\text{C}$, the microgels shrink slightly as T increases. However, when T increases from 31°C to 35°C , the microgel particles undergo a dramatic, but continuous, volume change. The phase transition temperature of the microgels is $\sim 33.0^\circ\text{C}$ similar to that of individual PNIPAM linear chains in water. Further increase of temperature has little effect on $\langle R_h \rangle$. On the basis of the temperature dependence of $\langle R_h \rangle$, we used static LLS to characterize the PNIPAM microgels at three different temperatures, corresponding to three different stages of the swelling and collapse of the microgels.

Table 1 summarizes the results of static LLS measurements at two different temperatures. The large dn/dC increase from 0.181 mL g^{-1} at $T = 30^\circ\text{C}$ to 0.201 mL g^{-1} at $T = 35^\circ\text{C}$ is attributed to the increase in the PNIPAM chain segment density ρ from 0.021 g cm^{-3} to 0.30 g cm^{-3} . The decrease of $\langle R_g \rangle$ reflects the collapse of the microgels. The change of A_2 from positive to negative indicates that water becomes a poor solvent at 35°C , just as for individual PNIPAM chains in water. The Θ -temperature ($\sim 31^\circ\text{C}$) of the PNIPAM microgel in water, as estimated from the temperature dependence of A_2 , was similar to that of individual chains. On the basis of the values of ρ and R_h listed in Table 1, we know that $\sim 94\%$ of water inside the swollen microgel network is driven out during the transition. The independence of M_w on temperature indicates that there is no aggregation.

In Table 1, the properties of the microgels are compared with those of linear PNIPAM chains whose M_w and M_w/M_n are $1.08 \times 10^7 \text{ g mol}^{-1}$ and 1.05 , respectively. For the PNIPAM microgels in water, $\langle R_g \rangle / \langle R_h \rangle$ ($\sim 0.78 \pm 0.03$) is very close to 0.774 predicted for a uniform hard sphere⁸⁰. The temperature independence of $\langle R_g \rangle / \langle R_h \rangle$ shows that even in the swollen state the microgels are spheres with a uniform density. The value of $\langle R_g \rangle / \langle R_h \rangle \sim 0.78$ also shows that the microgels are non-draining, i.e., all water molecules in the interior move together with the microgel network. The

constant value of $\langle R_g \rangle / \langle R_h \rangle$ suggests that the collapse of the microgels is uniform, which contracts with the behaviour of individual PNIPAM linear chains in water, where $\langle R_g \rangle / \langle R_h \rangle$ decreases dramatically from ~ 1.52 to ~ 0.65 in the same temperature range and the chain conformation changes from an extended coil to a collapsed globule.

Table 1 shows that the chain density ρ of the PNIPAM microgel network is only $\sim 0.30 \text{ g cm}^{-3}$ even in the collapsing limit, which is in agreement with that of bulk gels studied by small angle neutron scattering⁴³. This low chain density was explained by Grosberg *et al.*³⁹ in terms of the concept of the crumpled globule state. In comparison with the chain density ($\rho \sim 0.20 \text{ g cm}^{-3}$) of the PNIPAM linear chain in the globule state, the chain density of the microgel at its collapsing limit is slightly higher, but still much lower than the density ($\sim 1 \text{ g cm}^{-3}$) of bulk PNIPAM. In contrast, the chain density of the swollen microgel particles in the swollen state is ~ 4 times higher than that of the PNIPAM linear chains under the same conditions. This difference in the swelling capability can be better demonstrated by the expansion factor α .

Figure 13 shows temperature dependence of the expansion factor $\alpha_h[\equiv \langle R_h \rangle / \langle R_h \rangle_\Theta]$ as a function of temperature, where $\langle R_h \rangle_\Theta$ is the hydrodynamic radius at $T = \Theta$; 'O' represents for the PNIPAM linear chains ($M_w = 1.08 \times 10^7 \text{ g mol}^{-1}$ and $M_z/M_w < 1.05$) in water at $C = 4.60 \times 10^{-6} \text{ g mL}^{-1}$, and '□', for the microgels in water at $C = 1.18 \times 10^{-5} \text{ g mL}^{-1}$. Both of the volume changes are continuous. Several features in Figure 13 should be noted. First, as expected, the linear chains swell much more than the microgel particles in the good solvent region. Second, the phase transition of the microgel particles is less sharp. In the past, this less sharp phase transition was attributed to the irregularity of particle surface and the inhomogeneous particle size. This would make the phase transition of individual PNIPAM linear chains even less sharp because a linear chain has a wide distribution of chain conformations. We will come back to this point later. Third, the phase transition temperature of the microgel particles is $\sim 1.5^\circ\text{C}$ higher than that of the PNIPAM linear chains. Qualitatively, the higher phase transition temperature can also be explained on the basis of equations (1), (2) and (3). For the linear chains, $\Delta F = \Delta F_m$, while for the microgel particles, $\Delta F = \Delta F_m + \Delta F_{el}$. In a good solvent, $\Delta F < 0$ and both of the linear chains and the microgel particles are swollen. When $\Delta F > 0$, the segment-segment interaction is stronger than the solvent-segment interaction so that the linear chains and the microgels start to collapse. When a gel is swollen, $\alpha > 1$ and $\Delta F_{el} > 0$. The elasticity will retard the chain expansion in a good solvent. When a gel is collapsed, $\alpha < 1$ and $\Delta F_{el} < 0$. ΔF_{el} contributes negatively to ΔF and the elasticity prevents the gel collapse in a poor solvent. Therefore, the collapse of a linear chain is easier than that of a gel. It is known that ΔF_{el} is inversely proportional to the number of monomer units between two crosslinking points. This implies that in a poor solvent, the higher the crosslinking density (the smaller

Table 1 The laser light scattering results for the PNIPAM microgel particles in water at two different temperatures

T (°C)	Microgel particles						Linear chain			
	dn/dC ($\text{mL}\cdot\text{g}^{-1}$)	M_w (g/mol)	A_2 ($\text{mol}\cdot\text{mL}/\text{g}^2$)	R_g (nm)	R_h (nm)	R_g/R_h	ρ ($\text{g}\cdot\text{mL}^{-1}$)	R_g/R_h	ρ ($\text{g}\cdot\text{mL}^{-1}$)	dn/dC ($\text{mL}\cdot\text{g}^{-1}$)
30.01	0.181	2.19×10^8	3.02×10^{-6}	124	160	0.78	0.021	1.52	0.0063	0.167
35.01	0.201	2.25×10^8	-2.25×10^{-5}	57	70	0.81	0.30*	0.65*	0.20*	0.171*

*Represents the values at the collapsing limit.

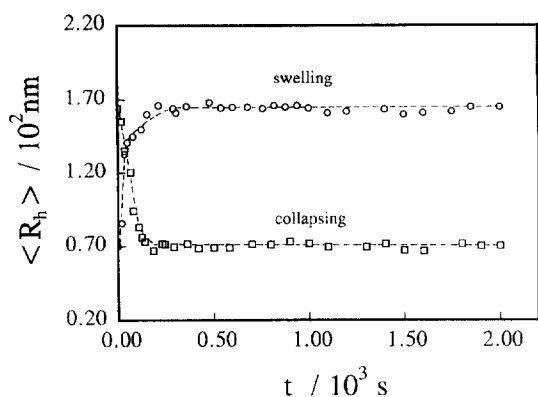


Figure 14 Collapsing and swelling kinetics of the PNIPAM microgel particles, after the temperature was abruptly changed from 30.0°C to 35.0°C, or *vice versa*⁸⁰

number), the higher the transition temperature, as experimentally confirmed⁷².

Figure 14 shows the collapsing and swelling kinetics (in terms of $\langle R_h \rangle$) of the microgels particles, where t is the standing time after the solution was quenched from 35.0°C to 30.0°C, or *vice versa*, from 30°C to 35°C. Both the swelling and collapse are too fast to be followed by our present LLS set-up. As stated before, for a spherical gel, $t = R^2/\pi^2 D$. Here, the hydrodynamic radius of the microgels at $T = \Theta$ is ~ 150 nm and the collective diffusion coefficient D_c is $\sim 10^{-7} \text{ cm}^2 \text{ s}^{-1}$, so that $t \sim 10^{-4}$ s. In comparison, the coil-to-globule transition of a high molar mass linear PNIPAM chain is much slower. This difference in the transition speed might also be due to the fact that the subchain between two crosslinking points in the microgel particles is $\sim 10^2$ times shorter than the length of the high molar mass linear PNIPAM chains. Moreover, the swelling or shrinking speed of a gel in response to an excess osmotic pressure is controlled by the collective diffusion of solvent into the gel. A very large surface-to-volume ratio of the microgels leads to a very fast swelling or shrinking in comparison with bulk gels.

The next question is whether the volume phase transition is discontinuous or continuous. The shrinking of the linear chains and spherical microgels can be better viewed in terms of α_b , as shown in Figure 13. At 20°C, the swelling of the microgels is much less than the linear chains. As stated before, for both of these cases, the volume changes are continuous. It is well known that for a linear polymer chain in solution its phase transition temperature varies with its

molar mass⁶⁰. For a given polymer solution with an LCST, the higher the molar mass the lower the phase transition temperature. Therefore, for a polydisperse sample the polymer chains with different lengths undergo the phase transition at different temperatures, which smears the volume phase transition, so that the phase transition of individual linear PNIPAM chains becomes continuous (Figure 13) even though the volume phase transition observed in this study is already much sharper than any previously reported results. As expected, only can a monodisperse polymer chain display a discontinuous phase transition. It should be noted that Grosberg *et al.*⁴ predict the sharpness of the 'coil-to-globule' transition is dependent of $(A_3/a^6)^{1/2}$, namely if $(A_3/a^6)^{1/2}$ is smaller than 0.05 the transition will be the first order (sharp); otherwise, the transition will be the second order (smooth), where A_3 is the third virial coefficient and a is the statistical segment of the chain. Our previous study showed that even at 20°C which is far away from the Flory Θ -temperature ($\sim 30.59^\circ\text{C}$) the value of A_2 is only in the order of 10^{-5} and the value of A_3 is practically zero. It is expected that when the 'coil-to-globule' transition temperature (31.8°C) is very close to the Θ -temperature the value of A_3 will be even smaller. Therefore, the ratio of $(A_3/a^6)^{1/2}$ must be very small.

Figure 13 shows that the linear chains have a sharper volume change and a lower transition temperature than the microgels. Tanaka *et al.*⁷ have attributed this less sharper volume change to the microgel's polydispersity. However, according to equations (6) and (7), the transition temperature (equivalently χ_T) is not related to the gel dimension because temperature is a thermodynamic intensive property. In contrast, χ_T or the phase transition temperature, is directly related to the subchain length or M_c .

Figure 15 shows a simulation of χ_T versus ϕ on the basis of equations (6) and (7) whereby χ_T decreases as ζ decreases, i.e., as M_c decreases. Note that for a polymer gel with an LCST a higher χ_T means a higher temperature. Therefore, the transition temperature decreases as M_c increases. On the basis of this M_c -dependence of χ_T , it becomes clear that the linear chains have a lower transition temperature because its average molar mass ($M_w = 1.08 \times 10^7 \text{ g mol}^{-1}$) is much higher than that of the subchains ($M_c \sim 10^4 \text{ g mol}^{-1}$).

Normally, the subchains inside a polymer gel have a broad molar mass (length) distribution and a gel network can be visualized as a set of sub-networks with each sub-network having a different M_c . As temperature changes, the sub-network with a longer subchain will undergo the phase transition before the sub-network with a short subchain. Thus, different parts of the gel network undergo the phase transition at different temperatures. The fact that a transparent PNIPAM gel changes into a milky gel in the phase transition indicates this microscopic inhomogeneity. Therefore, the volume phase transition of a polymer gel should be practically continuous because the subchains normally have a broad chain length distribution.

Conceptually, the discontinuous volume phase transition predicted on the basis of equations (7) and (8) is correct if M_c is a constant. However, it will be extremely difficult, if not impossible, to prepare such a polymer gel. In contrast, it is fair to state that using one average M_c was very successful in many other predictions, e.g., in the relation between a shear modulus G and M_c , i.e. $G = RT\rho\phi/M_c$, where ϕ is the volume ratio of the dry and swollen gel.

For a discontinuous volume phase transition observed in

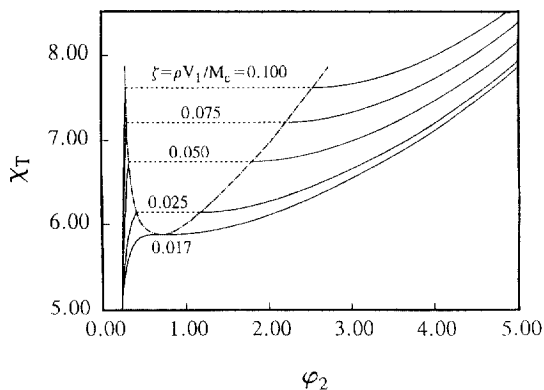


Figure 15 Plot of χ_T versus ϕ_2 for a polymer gel on the basis of equations (7) and (8), wherein we have chosen $k = 0.5$, $(\alpha^2) = 0.04$ and $\zeta = \rho V_1/M_c$ (see equations (7) and 8)⁸⁶

bulk PNIPAM gels, a possible explanation is as follows. As discussed earlier, longer subchains inside the gel undergo the phase transition before shorter subchains. Therefore, the shrinking of small amount of longer subchains initially will not alert the overall dimension of a bulk gel because of its shear module, but can build up stress inside the gel. When temperature increases, the stress will gradually increase until the shear module cannot maintain the macroscopic shape of the gel and the overall dimension of the gel will change abruptly, i.e., a discontinuous macroscopic volume change. As for the microgels with an average radius of $\sim 0.1\text{--}0.2\mu\text{m}$, the shear module plays a minor role so that its dimension changes continuously when the stress increases. It is known^{83,84} that a very long time (a few days) is needed for a bulk gel to reach its true swelling or shrinking equilibrium. For such a long time period, the temperature has to be kept constant (e.g. $\pm 0.01^\circ\text{C}$ in this study) and the incremental temperature change has to be less than 0.1°C . Otherwise, a continuous volume phase change could be interpreted as a discontinuous one. In contrast, the study of the microgels is more straightforward because they can reach the equilibrium in less than 1 s.

CONCLUSION

With the success of preparing two narrowly distributed high molar mass poly(N-isopropylacrylamide) (PNIPAM), we have accomplished the studies of the coil-to-globule transition of individual PNIPAM chain in extremely dilute solution. We have, for the first time, demonstrated that a thermodynamically stable single-chain globule state can be experimentally reached. Our results showed that R_g/R_h decreases linearly as temperature increases when $T > \Theta$. Our results also showed that in the coil-to-globule transition R_g/R_h can be lower than 0.774 predicted for a uniform sphere, indicating that the transition is not an 'all-or-nothing' process, and in the globular state the chain density is not uniform. The observed time scale ($\sim 10^2$ s) for the coil-to-globule transition of a very long PNIPAM chain was too short to support the previously proposed the knotting of the chain inside the globule. In addition, the highest chain density reached in the collapsed globule is only 0.2 g cm^{-3} which is significantly lower than that in bulk ($\sim 1\text{ g cm}^{-3}$), implying that the collapsed globule still contains $\sim 80\%$ water. Finally, our results in terms of both the expansion (or say contraction) factor α and the scaled expansion factor $\alpha^3 \tau M_w^{1/2}$ indicate that the modified Flory theory for the polymer chain expansion (contraction) works well in a good solvent and near the Θ -temperature, but failed in the region where the chain is highly collapsed. The theory has to be further modified to include the strong attractive interaction inside the globule.

ACKNOWLEDGEMENTS

The financial support of the RGC (Research Grants Council of Hong Kong) Earmarked Grant 1995/96 (CUHK 305/96P, 2160063) is gratefully acknowledged.

REFERENCES

1. Stockmayer, W. H., *Makromol. Chem.*, 1960, **35**, 54.
2. Ptitsyn, O. B., Kron, A. K. and Eizner, Y. Y., *J. Polym. Sci., Part C*, 1968, **16**, 3509.
3. Yamakawa, H., *Modern Theory of Polymer Solutions*, Harper and Row, New York, 1971.
4. Grosberg, A. Y. and Kuznetsov, D. V., *Macromolecules*, 1992, **25**, 1996.
5. Yamakawa, H., *Macromolecules*, 1993, **26**, 5061.
6. Post, C. B. and Zimm, B. H., *Biopolymers*, 1979, **18**, 1487; 1982, **21**, 2123.
7. Park, I. H., Wang, Q. W. and Chu, B., *Macromolecules*, 1987, **20**, 1965.
8. Chu, B., Park, I. H., Wang, Q. W. and Wu, C., *Macromolecules*, 1987, **20**, 2883.
9. Chu, B., Yu, J. and Wang, Z. L., *Prog. Colloid Poly. Sci.*, 1993, **91**, 142.
10. Tanaka, F., *J. Chem. Phys.*, 1985, **85**, 4707.
11. Lerman, L. S., *Proc. Natl. Acad. Sci. USA*, 1971, **68**, 1886.
12. Grosberg, A. Y. and Kuznetsov, D. V., *Macromolecules*, 1993, **26**, 4249.
13. Yu, J., Wang, Z. L. and Chu, B., *Macromolecules*, 1992, **25**, 1618.
14. Chu, B., Ying, Q. C. and Grosberg, A. Y., *Macromolecules*, 1995, **28**, 180.
15. Chan, H. S. and Dill, K. A., *Physics Today*, 1993, **46**, 24.
16. Post, C. B. and Zimm, B. H., *Biopolymers*, 1982, **21**, 2139.
17. Lerman, L. S., *Proc. Natl. Acad. Sci. USA*, 1971, **68**, 1886.
18. Lerman, L. S. and Allen, S. L., *Cold Spring Harbor Symp. Quant. Biol.*, 1973, **38**, 59.
19. Yamamoto, I., Iwasaki, K. and Hirotsu, S., *J. Phys. Soc. Japan*, 1989, **58**, 210.
20. Kubota, K., Fujishige, S. and Ando, I., *J. Phys. Chem.*, 1990, **94**, 5154.
21. Meewes, M., Ricka, J., de Silva, M. and Binkert, Th., *Macromolecules*, 1991, **24**, 5811.
22. Schild, H. G., *Prog. Polym. Sci.*, 1992, **17**, 163.
23. Dusek, K. and Patterson, D., *J. Polym. Sci., Phys. Ed.*, 1968, **6**, 1209.
24. Hasa, J., Ilavsky, M. and Dusek, K., *J. Polym. Sci., Polym. Phys. Ed.*, 1975, **13**, 253.
25. Tanaka, T., *ACS Symp. Ser.*, 1991, **480**, 1.
26. Shibayama, M. and Tanaka, T., *Advances in Polym. Sci.*, 1993, **109**, 1.
27. Osada, Y. and Ross-Murphy, S. B., *Sci. Am.*, 1993, **264**, 42.
28. Ilavsky, M., *Macromolecules*, 1982, **15**, 782.
29. Tanaka, T., Fillmore, D., Sun, S. T., Nishio, I. and Suislow, G., *Phys. Rev. Lett.*, 1980, **45**, 1636.
30. Tanaka, T., Nishio, I., Sun, S. T. and Nishio, S. U., *Science*, 1982, **218**, 467.
31. Suzuki, A. and Tanaka, T., *Nature*, 1990, **346**, 345.
32. Erman, B. and Flory, P. J., *Macromolecules*, 1986, **19**, 2342.
33. Hirokawa, Y., Tanaka, T. and Matsuo, E. S., *J. Chem. Phys.*, 1984, **81**, 6379.
34. Freitas, R. F. S. and Cussler, E. L., *Sep. Sci. Technol.*, 1987, **22**, 911.
35. Hirotsu, S., Hirokawa, Y. and Tanaka, T., *J. Chem. Phys.*, 1987, **87**, 1392.
36. Hirotsu, S., *Adv. Polym. Sci.*, 1993, **110**, 1.
37. Otake, K., Inomata, H., Konno, M. and Saito, S., *J. Chem. Phys.*, 1990, **91**, 1345.
38. Marchetti, M., Prager, S. and Cussler, E. L., *Macromolecules*, 1990, **23**, 1760, 3445.
39. Grosberg, A. Yu. and Nechaev, S. K., *Macromolecules*, 1991, **24**, 2789.
40. Otake, K., Inomata, H., Konno, M. and Saito, S., *Macromolecules*, 1990, **23**, 283.
41. Hirokawa, Y., Sato, E., Hirotsu, S. and Tanaka, T., *Polym. Mater. Sci. Eng.*, 1985, **52**, 520.
42. Li, Y. and Tanaka, T., *J. Chem. Phys.*, 1989, **90**, 5161.
43. Tokita, M. and Tanaka, T., *Science*, 1991, **253**, 1121.
44. Shibayama, M. and Tanaka, T., *J. Chem. Phys.*, 1992, **97**, 6829.
45. Badiger, M. V., Rajamohanam, P. R., Kulkarni, M. G., Ganapathy, S. and Mashelkar, R. V., *Macromolecules*, 1991, **24**, 106.
46. Tanaka, T., Sato, E., Hirokawa, Y., Hirotsu, S. and Peetermans, J., *Phys. Rev. Lett.*, 1985, **55**, 2455.
47. Sato, E. and Tanaka, T., *J. Chem. Phys.*, 1988, **89**, 1695.
48. Hirose, Y., Amiya, T., Hirokawa, Y. and Tanaka, T., *Macromolecules*, 1987, **20**, 1342.
49. Snowden, M. J., Vincent, B. and Morgan, J. C., UK Pat. GB2262117A, 1993.
50. Pelton, R. H. and Chibante, P., *Colloids Surf.*, 1986, **20**, 247.
51. McPhee, W., Tam, K. C. and Pelton, R. H., *J. Colloid and Interface Sci.*, 1993, **156**, 24.
52. Murray, M., Rana, F., Haq, I., Cook, J., Chowdhry, B. Z. and Snowden, M. J., *J. Chem. Soc., Chem. Comm.*, 1994, **18**, 1803.
53. Rodriguez, B. E. and Wolfe, M. S., *Macromolecules*, 1994, **27**, 6642.
54. de Gennes, P. G., *J. Phys. Lett.*, 1975, **36**, L55.
55. Sanchez, I. C., *Macromolecules*, 1979, **12**, 276.

56. Akcasu, A. Z. and Han, C. C., *Macromolecules*, 1979, **12**, 980.
57. Chan, H. S. and Dill, K. A., *J. Chem. Phys.*, 1994, **100**, 9238.
58. de Gennes, P. G., *J. Phys. Lett.*, 1985, **46**, L-639.
59. Grosberg, A. Yu., Nechaev, S. K. and Shakhovich, E., *J. Phys. Fr.*, 1988, **49**, 2095.
60. Flory, P. J., *Principles of Polymer Chemistry*, Cornell University Press, New York, 1953.
61. Flory, P. J., *J. Am. Chem. Soc.*, 1956, **78**, 5222.
62. Hermans, J. J., *J. Polym. Sci.*, 1956, **59**, 191.
63. James, H. M. and Guth, E., *J. Chem. Phys.*, 1953, **21**, 1048.
64. Dusek, K. and Prins, W., *Adv. Polym. Sci.*, 1969, **6**, 1.
65. Hirotsu, S., *J. Phys. Soc. Japan*, 1987, **56**, 233.
66. Hirose, Y., Hirokawa, Y. and Tanaka, T., *Macromolecules*, 1987, **20**, 1342.
67. Marchetti, M., Prager, S. and Cussler, E. L., *Macromolecules*, 1990, **23**, 3445.
68. Inomata, H., Goto, S. and Saito, S., *Macromolecules*, 1990, **23**, 4888.
69. Kokufuta, E., Zhang, Y. and Tanaka, T., *Macromolecules*, 1993, **26**, 1053.
70. Shibayama, M., Morimoto, M. and Nomura, S., *Macromolecules*, 1994, **27**, 5060.
71. Park, T. G. and Hoffman, A. S., *J. Appl. Polym. Sci.*, 1994, **52**, 85.
72. Yu, H. and Grainger, D. W., *Macromolecules*, 1994, **27**, 4554.
73. Zimm, B. H., *J. Chem. Phys.*, 1948, **16**, 1099.
74. Debye, P., *J. Phys. and Coll. Chem.*, 1947, **51**, 18.
75. Pecora, R., *Dynamic Light Scattering*, Plenum Press, New York, 1976.
76. Chu, B., *Laser Light Scattering*, 2nd edn. Academic Press, New York, 1991.
77. Stockmayer, W. H. and Schmidt, M., *Pure Appl. Chem.*, 1982, **54**, 407; *Macromolecules*, 1984, **17**, 509.
78. Zhou, S. Q., Fan, S. Y., Au-yeung, S. T. F. and Wu, C., *Polymer*, 1995, **36**, 1341.
79. Wu, C. and Zhou, S. Q., *Macromolecules*, 1995, **28**, 5388.
80. Wu, C. and Zhou, S. Q., *J. Polym. Sci., Polym. Phys. Ed.*, 1996, **34**, 1579.
81. Wu, C., Chan, K. and Xia, K. Q., *Macromolecules*, 1995, **28**, 1032.
82. Wu, C. and Zhou, S. Q., *Phys. Rev. Lett.*, 1996, **77**, 3053.
83. Wu, C. and Yan, C. Y., *Macromolecules*, 1994, **27**, 4516.
84. Wu, C. and Zhou, S. Q., *Macromolecules*, 1996, **29**, 4998.
85. Wu, C. and Zhou, S. Q., *Macromolecules*, 1995, **28**, 8381.
86. Wu, C. and Zhou, S. Q., *Macromolecules*, 1997, **30**, 574.